ORIGINAL ARTICLE

Journal of Cachexia, Sarcopenia and Muscle 2024; **15**: 989–1002
Published online 14 May 2024 in Wiley Online Library (wileyonlinelibrary.com) **DOI:** 10.1002/jcsm.13468

Skeletal muscle hypertrophy rewires glucose metabolism: An experimental investigation and systematic review

Philipp Baumert[1,2,3]*, Sakari Mäntyselkä[4], Martin Schönfelder[1], Marie Heiber[1,5], Mika Jos Jacobs[1], Anandini Swaminathan[6], Petras Minderis[6], Mantas Dirmontas[7], Karin Kleigrewe[8], Chen Meng[8], Michael Gigl[8], Ildus I. Ahmetov[2], Tomas Venckunas[6], Hans Degens[6,9], Aivaras Ratkevicius[6,10], Juha J. Hulmi[4] & Henning Wackerhage[1]

[1]*School of Medicine and Health, Technical University of Munich, Munich, Germany;* [2]*Research Institute for Sport and Exercise Sciences, Liverpool John Moores University, Liverpool, UK;* [3]*Research Unit for Orthopaedic Sports Medicine and Injury Prevention (OSMI), UMIT TIROL - Private University for Health Sciences and Health Technology, Innsbruck, Austria;* [4]*Faculty of Sport and Health Sciences, NeuroMuscular Research Center, University of Jyväskylä, Jyväskylä, Finland;* [5]*Institute of Sport Science, University of the Bundeswehr Munich, Neubiberg, Germany;* [6]*Institute of Sport Science and Innovations, Lithuanian Sports University, Kaunas, Lithuania;* [7]*Department of Health Promotion and Rehabilitation, Lithuanian Sports University, Kaunas, Lithuania;* [8]*Bavarian Center for Biomolecular Mass Spectrometry, Technical University of Munich, Munich, Germany;* [9]*Department of Life Sciences, Manchester Metropolitan University, Manchester, UK;* [10]*Sports and Exercise Medicine Centre, Queen Mary University of London, London, UK*

Abstract

Background Proliferating cancer cells shift their metabolism towards glycolysis, even in the presence of oxygen, to especially generate glycolytic intermediates as substrates for anabolic reactions. We hypothesize that a similar metabolic remodelling occurs during skeletal muscle hypertrophy.

Methods We used mass spectrometry in hypertrophying C2C12 myotubes in vitro and plantaris mouse muscle in vivo and assessed metabolomic changes and the incorporation of the [U-$^{13}C_6$]glucose tracer. We performed enzyme inhibition of the key serine synthesis pathway enzyme phosphoglycerate dehydrogenase (Phgdh) for further mechanistic analysis and conducted a systematic review to align any changes in metabolomics during muscle growth with published findings. Finally, the UK Biobank was used to link the findings to population level.

Results The metabolomics analysis in myotubes revealed insulin-like growth factor-1 (IGF-1)-induced altered metabolite concentrations in anabolic pathways such as pentose phosphate (ribose-5-phosphate/ribulose-5-phosphate: +40%; $P = 0.01$) and serine synthesis pathway (serine: −36.8%; $P = 0.009$). Like the hypertrophy stimulation with IGF-1 in myotubes in vitro, the concentration of the dipeptide L-carnosine was decreased by 26.6% ($P = 0.001$) during skeletal muscle growth in vivo. However, phosphorylated sugar (glucose-6-phosphate, fructose-6-phosphate or glucose-1-phosphate) decreased by 32.2% ($P = 0.004$) in the overloaded muscle in vivo while increasing in the IGF-1-stimulated myotubes in vitro. The systematic review revealed that 10 metabolites linked to muscle hypertrophy were directly associated with glycolysis and its interconnected anabolic pathways. We demonstrated that labelled carbon from [U-$^{13}C_6$]glucose is increasingly incorporated by ∼13% ($P = 0.001$) into the non-essential amino acids in hypertrophying myotubes, which is accompanied by an increased depletion of media serine ($P = 0.006$). The inhibition of Phgdh suppressed muscle protein synthesis in growing myotubes by 58.1% ($P < 0.001$), highlighting the importance of the serine synthesis pathway for maintaining muscle size. Utilizing data from the UK Biobank ($n = 450\,243$), we then discerned genetic variations linked to the serine synthesis pathway (*PHGDH* and *PSPH*) and to its downstream enzyme (*SHMT1*), revealing their association with appendicular lean mass in humans ($P < 5.0e\text{-}8$).

Conclusions Understanding the mechanisms that regulate skeletal muscle mass will help in developing effective treatments for muscle weakness. Our results provide evidence for the metabolic rewiring of glycolytic intermediates into anabolic pathways during muscle growth, such as in serine synthesis.

Keywords lactate; metabolomics; resistance exercise; serine synthesis pathway; Warburg effect

Received: 23 December 2022; Revised: 6 February 2024; Accepted: 15 March 2024
*Correspondence to: Philipp Baumert, School of Medicine and Health, Technical University of Munich, Munich, Germany. Email: philipp.baumert@tum.de
Sakari Mäntyselkä and Martin Schönfelder shared second authorship, and both authors contributed equally to this work.
Juha J. Hulmi and Henning Wackerhage shared senior authorship, and both authors contributed equally to this work.

Introduction

Muscle hypertrophy and increased strength are typical adaptations to resistance training or chronic muscle overload in mice.[1] Resistance training is an effective, low-cost intervention for the prevention and treatment of muscle loss in healthy and diseased individuals.[2] Resistance training not only increases muscle size and strength but also improves glycaemic control, increases glucose uptake and increases insulin sensitivity, suggesting metabolic adaptations in healthy as well as diabetic people. While the mechanistic target of rapamycin complex 1 (mTORC1) has been identified as a key mediator of increased protein synthesis after resistance exercise and during chronic overload,[3] there are still many gaps in our understanding of how changes in the muscle metabolism possibly contribute to muscle hypertrophy[1] or atrophy.[4]

Research especially on cancer shows that proliferating cells reprogram their metabolism and synthesize lactate in the presence of oxygen, which has been termed the Warburg effect. One key function of the Warburg effect is to synthesize glycolytic metabolites as substrates for anabolic reactions that build biomass.[5] About 20% of the carbon dry mass of cancer cells is delivered from glucose carbon,[6] which is accomplished by directing some glycolytic intermediates towards anabolic pathways such as the serine synthesis and pentose phosphate pathways. These two pathways generate critical precursors (e.g., non-essential amino acids and nucleotides) for the synthesis of macromolecules that are required for cancer cell proliferation.[7,8] Conversely, knockdown of the key enzyme phosphoglycerate dehydrogenase (Phgdh), which diverts the glucose-derived 3-phosphoglycerate away from glycolysis into the de novo serine synthesis pathway, reduces cancer cell proliferation,[9] indicating the importance of this pathway for cellular growth and proliferation. We recently hypothesized that Warburg-like metabolic reprogramming also occurs in mature, hypertrophying muscle fibres.[10] Consistent with this, several investigations indicate increased expression of genes that encode enzymes of anabolic pathways[11,12] and a rewiring of glucose metabolism in hypertrophying muscles.[13–16]

In this study, by using a mass spectrometry-based metabolomics approach in hypertrophy-stimulated muscles both in C2C12 myotubes in vitro and in plantaris mouse muscle in vivo, we identified metabolite level changes linked to the pentose phosphate and serine synthesis pathways in hypertrophy-stimulated muscles. We additionally analysed pre-existing metabolomics datasets in mice and utilized the UK Biobank to identify genetic variations and their association with human appendicular lean mass, further indicating a role of metabolic pathways parallel to glycolysis in muscle growth. A stable isotope [U-$^{13}C_6$]glucose tracer revealed that the carbon of glucose is increasingly incorporated into non-essential amino acids during muscle growth. Finally, we inhibited the key enzyme of the serine synthesis pathway in differentiated muscle cells, revealing an important role of this pathway in protein synthesis. Our results further demonstrate that hypertrophying skeletal muscle reprograms its metabolism to support biomass production.

Material and methods

Animals and in vivo study design

All procedures involving mice were approved by the Lithuanian State Food and Veterinary Service (Animal Ethics Number: 2018-06-14, Nr. G2-90). Male C57BL/6J mice were used in all experiments. Mice were housed in standard cages, one to three mice per cage, at a temperature of 22–24°C and 40–60% humidity. Animals were fed a standard chow diet and received tap water ad libitum.

Six mice were subjected to muscle overload of the plantaris muscle for 14 days, starting at the age of 32 weeks. After cessation of nociceptive responses, an incision was made in the popliteal area of the left hind limb to expose the tibial nerve with blunt dissection. The branches of the tibial nerve that innervate the soleus and gastrocnemius muscles were cut and small segments removed to prevent reinnervation. This strategy imposes an overload and subsequent compensatory hypertrophy of the plantaris muscle. The contralateral plantaris muscle of these mice served as an internal control in the analysis of muscle mass and metabolomics measurements. After 14 days, mice were fasted overnight, and they were sacrificed by exposure to CO_2. Immediately after sacrifice, the plantaris muscle was excised, blotted dry, weighed and frozen in isopentane (pre-cooled with liquid nitrogen). The muscle was then stored at −80°C until further metabolomics analysis. For a detailed description, see supporting information.

Cell culture and in vitro study design

Mouse C2C12 myoblast cells were cultured in Dulbecco's modified Eagle's medium (DMEM) supplemented with 10%

foetal bovine serum (FBS). To induce differentiation, the myoblasts were cultured until confluence, and then the medium was switched to DMEM with 0.2% FBS. After 72 h of differentiation, C2C12 myotubes were serum starved (DMEM only) for 4 h and then treated with DMEM including 0.2% dialysed FBS and vehicle control (10 mM of HCL, 0.1% bovine serum albumin [BSA]), insulin-like growth factor-1 (IGF-1; 100 ng/mL; recombinant Human LONG R^3 IGF-1, Sigma-Aldrich, Cat# I1271, MO, USA), rapamycin (10 ng/mL; Calbiochem, Cat# 553210, Watford, Hertfordshire, UK) and IGF-1 + rapamycin for 48 h. For Phgdh inhibition experiments, we treated C2C12 cells for 48 h with the chemical PHGDH inhibitor NCT-503 (50 μM; MCE, HY-101966; MedChemExpress) 5 days after the initiation of differentiation in independent experiments to our recently published paper.[17] To measure carbon incorporation in IGF-1-stimulated C2C12 myotubes, 4.5 g/L glucose consisting of ~20% [U-$^{13}C_6$]glucose and 80% non-labelled glucose was added to glucose-free DMEM supplemented with 2% horse serum (Sigma-Aldrich, H1138, NY, USA). Cells were incubated for 24 h with isotope-enriched media on Day 3 post-differentiation, after which the media was collected. Finally, cells were harvested in 1 M of perchloric acid (PCA) for stable isotope analysis. Please see the supporting information for detailed experimental procedures.

RNA isolation, reverse transcription and quantitative real-time PCR

C2C12 myotubes were washed twice with phosphate-buffered saline (PBS) at room temperature and then lysed in lysis T buffer (Peqlab Biotechnology GmbH, Germany, Reference Number: 12-6634-01). Total RNA was then extracted with the peqGOLD Total RNA Kit C-Line (Peqlab Biotechnology GmbH, Reference Number: 12-6634-01) according to the manufacturer's instructions. For mRNA analysis, we synthesized cDNA using 2 μg of total RNA, and the cDNA was amplified with a PerfeCTa qPCR fluorescent SYBR Green SuperMix (Quantabio) using real-time quantitative PCR (Rotor-Gene RG 6000, QIAGEN). The primer sequences used for gene expression are shown in *Table S1*. Please see the supporting information for detailed experimental procedures.

Protein determination and western blot analysis

Cells were lysed on ice in 100 μL of radioimmunoprecipitation assay (RIPA) buffer, including 0.1% SDS, 0.5 M of sodium orthovanadate, 0.5% sodium deoxycholate, 50 mM of NaF, 1 mM of EDTA, 150 mM of NaCl, 1% Triton-X 100 and a 1X protease and phosphatase inhibitor cocktail (Peqlab Biotechnology GmbH). For the Phgdh inhibition experiment, protein synthesis in C2C12 myotubes was measured using the SUnSET protein synthesis measurement. Specific protein quantification was performed by western blot analysis. Protein samples containing 40 μg of protein were solubilized in Laemmli sample buffer containing 10% β-mercaptoethanol and heated for 5 min at 95°C. Samples were then separated by electrophoresis in a 10% SDS-PAGE gel (Bio-Rad, Germany). Proteins were transferred to polyvinylidene difluoride (PVDF) membranes (Bio-Rad) using a Trans-Blot Turbo Blotting System (Bio-Rad). After this, an antigen-blocking step (5% non-fat milk powder, 1X Tris-buffered saline, 1% Tween-20) was performed, and the PVDF membrane was then incubated overnight at 4°C with primary antibodies followed by secondary antibodies (see supporting information) for 1 h. The antibodies were detected using enhanced chemiluminescence (ECL) (Bio-Rad), and the signals were detected by an INTAS ChemoCam Imager (Royal Biotech GmbH, Germany). Immunoreactive bands were quantified using the ImageJ software (http://rsb.info.nih.gov/ij/index.html), and the strongest band at ~40 kDa of a Ponceau S stain of the membrane was used for normalization.[18] Please see the supporting information for detailed experimental procedures and included antibodies.

Metabolomics and gas chromatography mass spectrometry analysis

For untargeted metabolomics, differentiated muscle cells and plantaris muscle tissue were prepared based on Yuan et al.,[19] and a Nexera UHPLC system (Shimadzu, Nakagyo-ki, Kyoto, Japan) coupled with a Q-TOF mass spectrometer (TripleTOF 6600, AB Sciex, Framingham, MA, USA) was used. Separation of the samples was performed using a HILIC UPLC BEH Amide 2.1 × 100, 1.7 μm analytic column (Waters Corp., Milford, MA, USA) and a reversed-phase Kinetex XB-C18, 2.1 × 100, 1.7-μm analytical column (Phenomenex, Torrance, CA, USA), respectively. The ^{13}C labelling of the protein-bound alanine (product) was determined using gas chromatography-combustion-isotope ratio mass spectrometry (GC-C-IRMS) following derivatization as its MCME derivative. The media alanine (precursor) enrichment is determined by gas chromatography mass spectrometry. Unfortunately, we could not differentiate based on retention time, MS1 or fragmentation between glucose-6-phosphate, fructose-6-phosphate and glucose-1-phosphate, which is why we took them together and referred to them as phosphorylated sugar. Please see the supporting information for detailed experimental procedures.

Bioinformatics analysis of human data

Publicly available summary statistics[20] from the published genome-wide association study (GWAS) on appendicular lean mass of UK Biobank participants (n = 450 243)[21,22] were used

to identify possible associations ($P < 5.0e-8$) between single nucleotide polymorphisms (SNPs) located in or near genes involved in the regulation of the serine synthesis pathway and its downstream enzymes and appendicular lean mass. In the next step, the Genotype-Tissue Expression (GTEx) portal[23] was used to analyse the association between the lean mass-related SNPs and the expression of specific genes in different tissues ($P < 0.05$). Please see the supporting information for detailed experimental procedures.

Statistical analysis

Data are expressed as the mean ± standard error of the mean (SEM) for the indicated number of observations. Data were assessed for statistical significance by one-way or two-way analysis of variance (ANOVA) tests, followed by Tukey's honestly significant difference (HSD) or by using a two-tailed Student's *t*-test, as appropriate. A *P*-value of <0.05 was considered statistically significant. The reported unadjusted *P*-values for all metabolites in the cell culture study were subsequently adjusted to account for multiple hypothesis testing. The false discovery rate (FDR) method of Benjamini and Hochberg was used to perform the adjustment (FDR < 0.1). Unlike in vitro, we did not find significant results in the in vivo study after adjusting for multiple hypothesis testing FDR < 0.1. We therefore took metabolites into account in the in vivo study, which were significant after adjusting for multiple hypotheses testing FDR < 0.2 in vivo and were also significant in the in vitro experiment. The specific statistical tests that were used are indicated in the figure legend. Please see the supporting information for detailed experimental procedures.

Systematic review

This systematic review is registered on PROSPERO (Access Number: CRD42022318998; https://www.crd.york.ac.uk/PROSPERO/). One researcher searched in PubMed, Scopus and MetaboLights using the PICO framework, leading to the following search strategy: ([mice or mouse] and [metabolomics or metabolome or metabolomes] and [skeletal muscle]) and ([increase or increased or increases or increasing or increasingly] or [mass gain] or [hypertrophy]) until 11 May 2022. Two researchers then screened the search results. Two researchers individually assessed the quality of each individual study using the 10-item checklist of CAMARADES (Collaborative Approach to Meta-Analysis and Review of Animal Data from Experimental Studies) (*Table S2*). A metabolite set enrichment analysis was performed using the MetaboAnalyst 5.0 web platform. Please see the supporting information for detailed experimental procedures.

Results

Muscle growth stimulation with insulin-like growth factor-1 increases the concentration of most of the glycolytic intermediates in C2C12 myotubes

To study the metabolic consequences of stimulation and inhibition of muscle protein synthesis in differentiated C2C12 muscle cells in vitro, we treated myotubes with 100 ng/mL of IGF-1 and/or 10 ng/mL of rapamycin for 48 h. As expected, IGF-1 increased myotube diameter, whereas rapamycin prevented the increase induced by IGF-1 (ANOVA, all $P < 0.001$) (*Figure S1A*). Treatment with IGF-1 also increased the phosphorylation of the mTORC1 downstream target 70-kDa ribosomal protein S6 kinase (p70S6K) after 2 h (*Figure S1B*), which was accompanied 48 h later by accretion of protein mass (*Figure S1C*), implying a positive protein balance, while rapamycin completely abolished basal and IGF-1-stimulated phosphorylation of p70S6K.

Next, we analysed the metabolome of myotubes treated with vehicle control, IGF-1 or rapamycin for 48 h. We identified 155 metabolites from myotubes, of which 28 showed significant differences between IGF-1 and control, 60 between IGF-1 and rapamycin and 54 between the control and rapamycin groups, respectively (FDR < 0.1; *Figure 1A*). The principal component analysis of the three treatment groups showed a clear separation of the three experimental groups (*Figure 1B*). IGF-1 treatment changed the concentration of several amino acids (*Figure 1C*) and glycolytic metabolites (*Figures 2* and *S2A*).

To identify differences in the metabolism between scenarios of robust skeletal muscle growth and its absence, we conducted a metabolic set enrichment analysis of distinct metabolite concentrations subsequent to the administration of IGF-1 when compared with rapamycin (*Figure 1D*), IGF-1 compared with control (*Figure S2B*) and rapamycin compared with control (*Figure S2C*). These analyses were consistent with the Warburg effect. We then analysed the metabolic changes within the myotubes and focused on the metabolites that are associated with the glycolysis and its linked anabolic pathways, which had altered (FDR < 0.1) their concentration in response to IGF-1 or rapamycin treatment when compared with vehicle controls (*Figure 2* and *Tables S3C* and *S4C*). IGF-1 treatment significantly increased the concentration of lactate by 139% in myotubes ($P < 0.001$). With rapamycin treatment, the concentration of lactate decreased by 73.3% ($P = 0.002$). An elevation of lactate is caused by increased glycolysis, which is a phenomenon of the Warburg effect predominantly observed in cancer cells.[5] Concomitant with these changes, the concentration of phosphorylated sugar (the detection method used could not differentiate between glucose-6-phosphate, fructose-6-phosphate and glucose-1-phosphate) was higher by +27.5% ($P < 0.001$) and of ribose-5-phosphate/ribulose-5-phosphate of the pentose

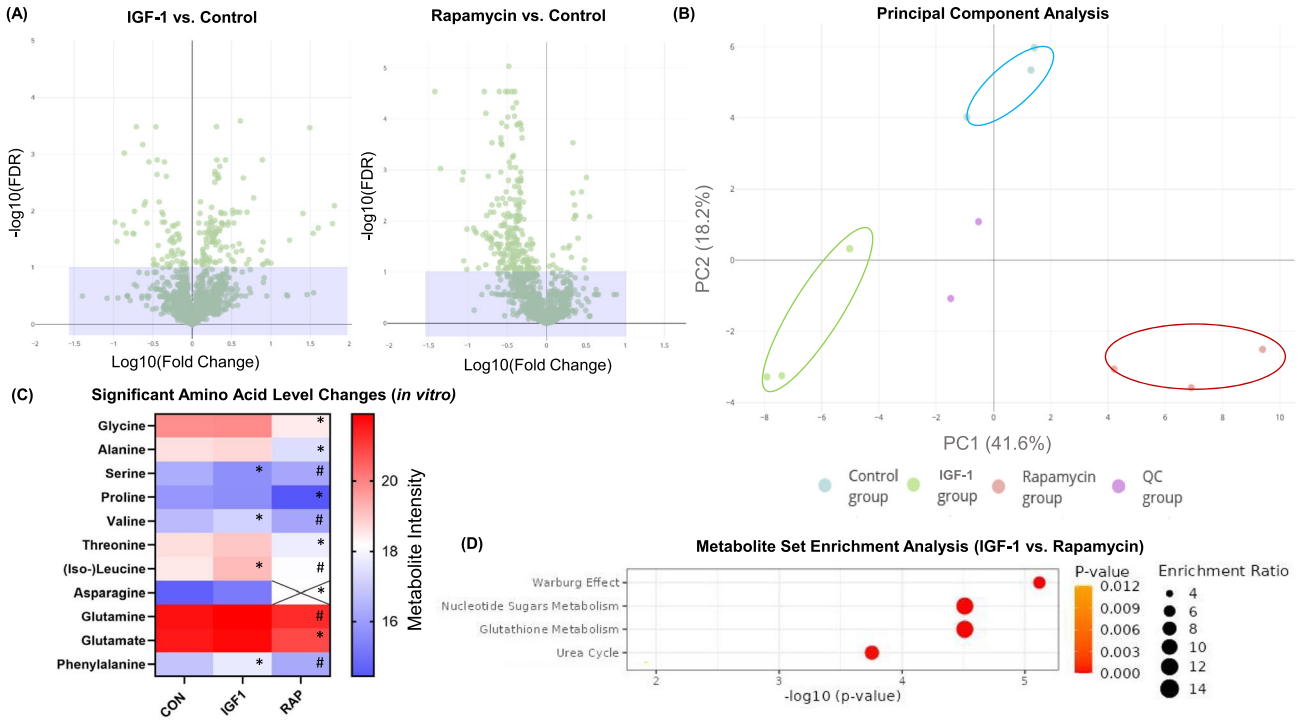

Figure 1 (A) Volcano plots displaying the false discovery rate (FDR) values (−log10) versus log10 fold changes of all features (i.e., both unannotated and annotated metabolites) of LC-MS/MS measurements (negative ion mode) between insulin-like growth factor-1 (IGF-1) and vehicle control (left) and between vehicle control and rapamycin (right) treatment in differentiated C2C12 muscle cells; features with FDR < 0.2 are above the purple box. (B) Principal component analysis (PCA) of metabolite intensities of LC-MS/MS measurements (negative ion mode). (C) Heatmap of significant amino acid level changes after vehicle control, IGF-1 or rapamycin treatment in vitro. Crosses indicate that the metabolite is below the detection limit. *Significant differences between treatments (IGF-1 or rapamycin) compared with vehicle control. #Significant differences between IGF-1 compared with rapamycin, unpaired two-tailed Student's *t*-test (FDR < 0.1). (D) Enrichment analysis with MetaboAnalyst 5.0 between IGF-1 and rapamycin treatments. CON, control; RAP, rapamycin.

phosphate pathway by +40% (P = 0.01) after IGF-1 treatment. Phosphorylated sugar was reduced by 71.4%, and ribose-5-phosphate/ribulose-5-phosphate and sedoheptulose-7-phosphate became undetectably low after rapamycin treatment (all $P < 0.001$; *Figure 2*). Of the 11 amino acids detected, IGF-1 treatment elevated the concentration of three (leucine/isoleucine, phenylalanine and valine) amino acids, and rapamycin reduced the concentration of six (alanine, asparagine, glycine, glutamate, proline and threonine) when compared with vehicle control (all $P < 0.01$; *Figure 1C*). Of the detected amino acids, only serine had a lower concentration in IGF-1-treated myotubes compared with vehicle control (−36.8%; P = 0.009). C2C12 myotubes consume rather than release serine into the media.[24] Thus, a decrease in serine concentration in the myotubes can be based on either a decreased activity of serine-producing enzymes or an elevated activity of serine-consuming enzymes.[25] The concentration of glycine (synthesized downstream of serine) did not change with IGF-1 treatment, and the concentration decreased by 64% when treated with rapamycin (P = 0.001). Thus, we assume that decreased serine concentration after IGF-1 treatment may indicate a high flux through the serine synthesis pathway due to an elevated demand for the glycine cleavage system, which refuels one-carbon metabolism.[26] Further, IGF-1 treatment increased metabolites linked to pyrimidine metabolism, that is, uridine 5′-monophosphate (+82%; P = 0.003) and uridine 5′-diphosphate (+130%; P = 0.004) compared with control treatment, whereas the former was decreased by 58.7% in the rapamycin group when compared with vehicle control (P = 0.016). The pyrimidine biosynthesis pathway is necessary for fundamental cellular functions such as DNA and RNA biosynthesis as well as glucose metabolism.

Unlike glycolytic intermediates, tricarboxylic acid (TCA) cycle metabolite concentrations changed little after IGF-1 treatment (*Tables S3* and *S4*). However, the intermediates fumarate and malate were decreased by ~70% in myotubes treated with rapamycin (both $P < 0.0025$; *Figure S2A*). Further, IGF-1 treatment increased the oxidized form of glutathione 10-fold, indicating that IGF-1-induced muscle hypertrophy may elevate oxidative stress in myotubes.

A small fraction of glucose from glycolysis can also be shuttled into the hexosamine biosynthetic pathway that generates uridine diphosphate (UDP)-sugar precursors. These activated sugars are required for an often overlooked post-translational modification called *O*-linked glycosylation.[27,28]

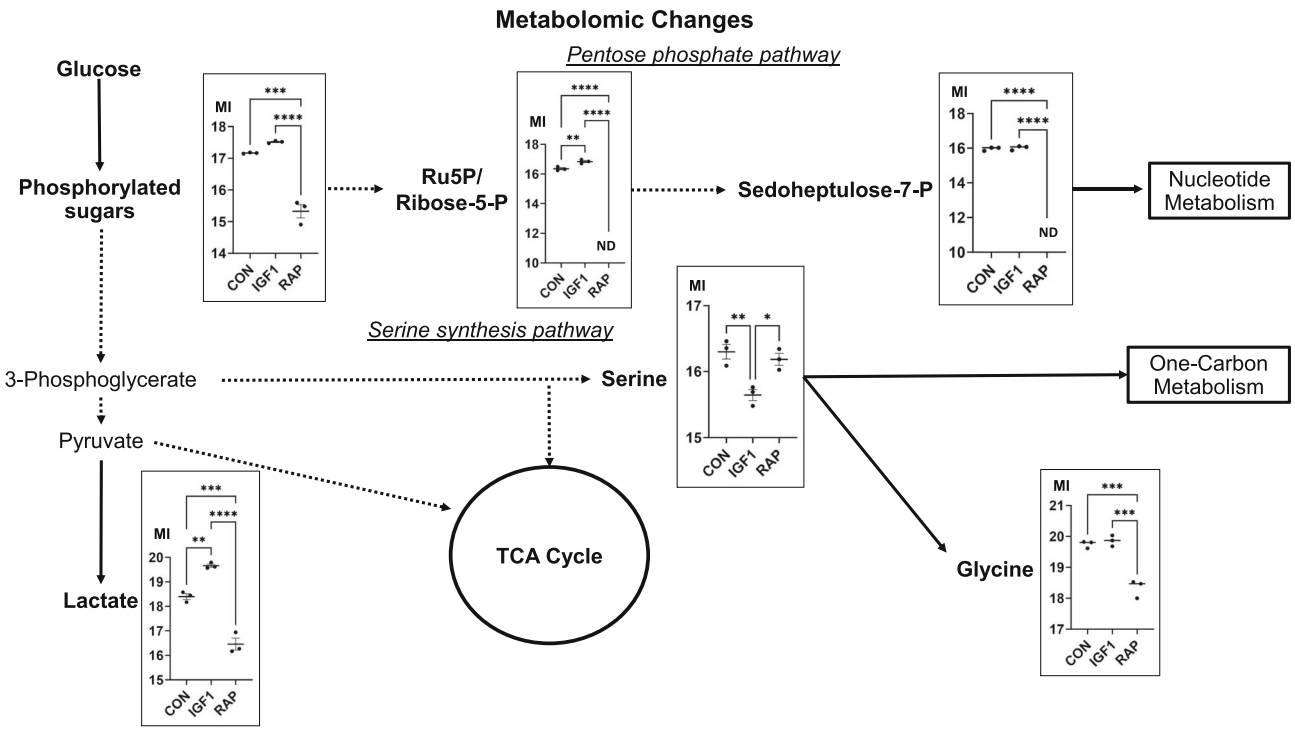

Figure 2 Metabolomic changes in differentiated C2C12 myotubes treated with vehicle control, insulin-like growth factor-1 (IGF-1; 100 ng/mL) or rapamycin (10 ng/mL) for 48 h (n = 3). Metabolites highlighted in bold were detected by untargeted metabolomics. Frames show significant metabolite level changes between conditions (FDR < 0.2). Metabolite intensity (MI) is represented on a $\log_2$ scale. CON, control; ND, not detected; P, phosphate; RAP, rapamycin; TCA, tricarboxylic acid cycle.

The metabolomics analysis also revealed changes in the metabolites of the hexosamine biosynthetic pathway (*Figure S3A*). Hypertrophy stimulation by IGF-1 treatment increased the concentration of nucleotide sugars, including UDP-*N*-acetylgalactosamine (UDP-GalNAc) (+76%) and UDP-glucuronic acid (+262%; both $P < 0.005$). By contrast, rapamycin treatment decreased the concentrations of UDP-glucuronic acid (−73.3%; P = 0.007), glucosamine-6-phosphate and UDP-galactose to levels under the detection limit.

To investigate whether the changes in metabolite concentrations were accompanied by changes in the expression of enzymes that synthesize or metabolize these metabolites, we measured the expression of genes that encode metabolic enzymes. Elevated gene expression of key enzymes of glycolysis and its parallel biomass pathways after treatment with IGF-I further supported the metabolic rewiring during skeletal muscle hypertrophy (*Figure 3A*). More specifically, glucose-6-phosphate dehydrogenase X (*G6pdx*), which encodes the rate-limiting enzyme of the oxidative pentose phosphate pathway, increased three-fold in response to IGF-1 treatment. The serine-pathway-related enzymes *Phgdh* and mitochondrial serine hydroxymethyltransferase-2 (*Shmt2*) also changed between the intervention groups, and especially *Shmt2* increased ~1.7-fold in abundance in hypertrophying muscle cells. The upregulation of these enzymes further suggests that the lower concentration of the serine metabolite mentioned above was indeed caused by an increased flux through the serine synthesis pathway. Given the significance of metabolites of the hexosamine pathway in our in vitro analysis, we also assessed the gene expression of *O*-glycosylation-related enzymes and the abundance of total glycosylated proteins in myotubes. However, we did not observe any significant differences between the groups at either the protein (*Figure S3B*) or gene level (*Figure S3C*).

To summarize, the data presented suggest that treating myotubes with IGF-1 results in metabolic reprogramming that enhances the use of glycolytic intermediates by anabolic pathways. Conversely, rapamycin decreases myotube anabolism, and this is accompanied by lower concentrations of metabolites involved in anabolic pathways.

Concentration of phosphorylated sugar also changes in hypertrophying murine muscle in vivo

To study the muscle metabolome response to a hypertrophic stimulus in vivo, we used an established muscle overload model.[29] Here, we induced compensatory hypertrophy of the right plantaris muscle in 8-month-old mice (n = 6; body weight = 31.3 ± 2.6 g) by denervation of gastrocnemius and soleus muscles. The advantage of this model is that the

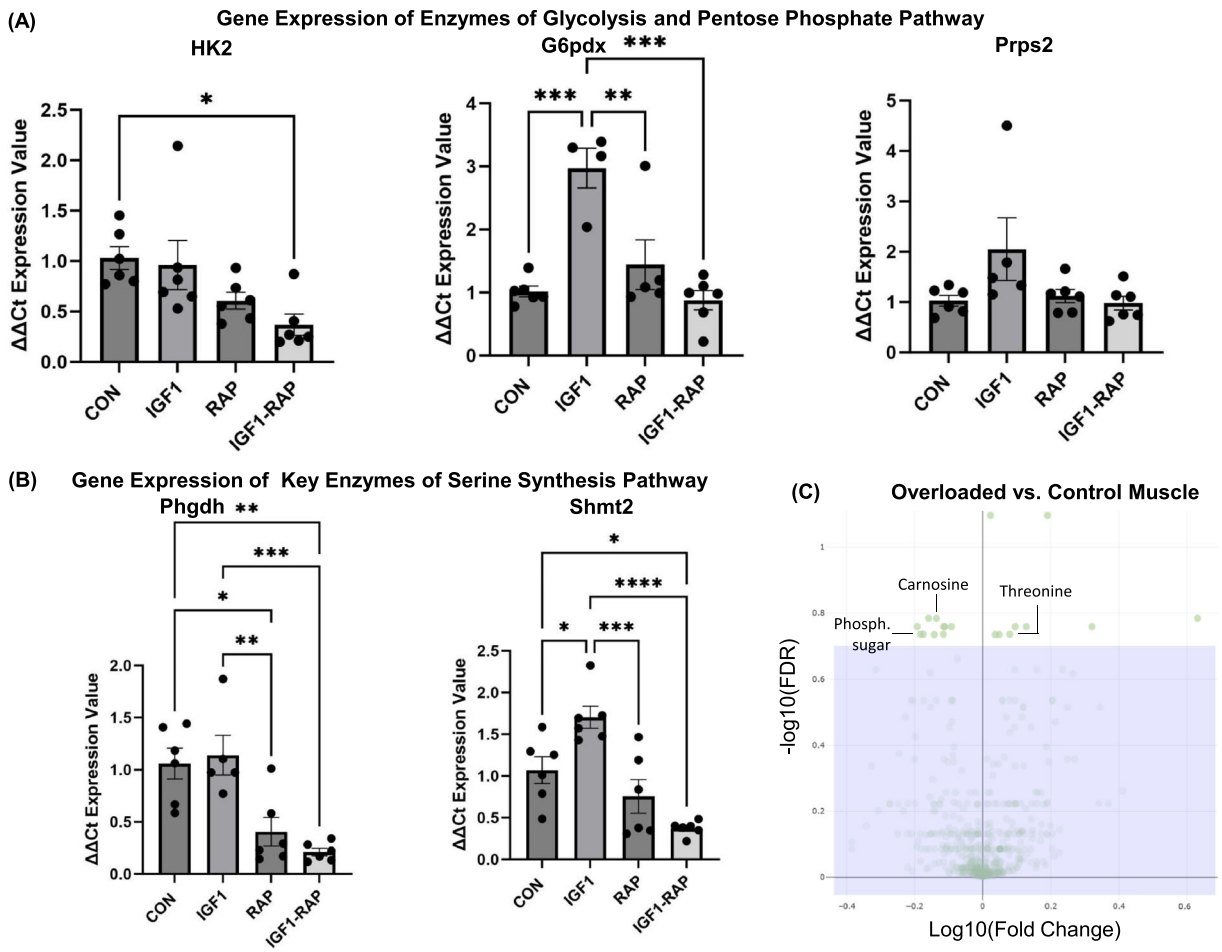

Figure 3 (A) Gene expressions of enzymes of glycolysis and the pentose phosphate pathway in C2C12 myotubes, including hexokinase 2 (Hk2), glucose-6-phosphate 1-dehydrogenase X (G6pdx) and phosphoribosyl pyrophosphate synthetase 2 (Prps2). (B) Gene expressions of key enzymes of the serine synthesis pathway in C2C12 myotubes: phosphoglycerate dehydrogenase (Phgdh) and serine hydroxymethyltransferase-2 (Shmt2). (C) Volcano plots displaying the false discovery rate (FDR) values (−log10) versus log10 fold changes of all features between overloaded and control mice plantaris muscles (negative ion mode); features with FDR < 0.2 are above the purple box. CON, control; IGF-1, insulin-like growth factor-1; Phosph. sugar, phosphorylated sugar; RAP, rapamycin. *Significant differences between indicated conditions, one-way ANOVA with Tukey's HSD post hoc test ($P < 0.05$). Data are expressed as the mean ± standard error of the mean (SEM).

plantaris muscle exhibits significant physiological hypertrophy by ~32% in 6 weeks[30] and yet is associated with less invasive surgery and an inflammatory response than during overload induced by ablation of synergists. We chose to examine the muscle metabolome at 14 days after denervation, at a time when there was yet only a small 13.5 ± 3.5% ($P = 0.007$) increase in skeletal muscle mass when compared with intact contralateral plantaris muscle, to capture a timepoint of physiological and stable active growth in muscle size.

After rapid quenching of the muscles, we determined metabolite concentrations using an untargeted liquid chromatography-tandem mass spectrometry (LC-MS/MS) method (FDR < 0.2; *Figure 3C*). Two metabolites exhibited alterations both in hypertrophied muscles in mice in vivo and in hypertrophying myotubes in vitro. Similar to the hypertrophy stimulation with IGF-1 in vitro, the concentration of the dipeptide L-carnosine (known for its antioxidant activity and antiglycation effects) was decreased by 26.6% ($P = 0.001$) during skeletal muscle growth in vivo (*Tables S5* and *S6*). However, phosphorylated sugar concentration showed contrasting trends, decreasing by 32.2% ($P = 0.004$) in the overloaded muscle in vivo while increasing in the IGF-1-stimulated myotubes in vitro, as mentioned before. When comparing the results of the in vivo muscle overload model with metabolite concentration changes between the hypertrophy-stimulating IGF-1 group and the absence of muscle growth represented by the rapamycin group in vitro, the concentration of threonine (in vivo +24.2%; $P = 0.009$) was increased in both experimental models of muscle hypertrophy. We also tested the total muscle *O*-*N*-acetylglucosamine (*O*-GlcNAc)-modified proteins in the in vivo overloaded plantaris muscles and could not find any differences compared with the control muscles ($P > 0.05$; *Figure S3D*).

Systematic review further demonstrates a metabolic rewiring of glycolytic intermediates in growing muscles

Currently, no single metabolomics methodology covers the complete collection of metabolites in tissue.[31] To address this issue, we compared our findings to previously published metabolomics datasets of in vitro murine muscle cells and in vivo murine experiments to gain a comprehensive insight into metabolomic changes during and after skeletal muscle hypertrophy. For this, we performed a systematic review (PROSPERO Access Number: CRD42022318998) following PRISMA guidelines[32] and searched the literature in three literature databases (PubMed, Scopus and MetaboLights) using the PICO framework. To assess the quality and risk of bias of the in vivo studies, the CAMARADES was used (*Table S2*). The results display metabolites that showed significantly changed concentrations in at least two experiments (*Figure S4*).

After removing duplicates, we screened 269 articles. Next to both present hypertrophying C2C12 muscle cells in vitro and plantaris muscle overload in vivo studies, we finally included another six publications that matched our eligibility criteria (see Material and Methods section), which investigated changes in the metabolome of skeletal muscle tissue in vivo or myotubes in vitro during skeletal muscle hypertrophy[13,14,33–36] (*Table 1*). We found 22 metabolites that were identified in at least two experiments (*Figure 4A*). About 73% of the observed metabolites that demonstrated changes in at least two experiments were detected in both study designs analysed either in hypertrophying mouse muscles in vivo or in growing differentiated muscle cells in vitro (*Figure 4B*). This confirms that in vitro studies mimic the metabolic response to muscle hypertrophy stimulation. These results align with gene expression outcomes, which also revealed a great overlap between bioengineered muscles compared with acute resistance exercise in humans.[37]

Ten of these 22 metabolites were directly related to glycolysis and its linked anabolic pathways. Generally, the concentrations of all included hexose phosphates (glucose-6-phosphate, fructose-6-phosphate and fructose-1,6-bisphosphate) were elevated in cell culture studies in vitro. However, the prevailing trend was a decrease in these concentrations in in vivo hypertrophying mouse muscles. Ribose-5-phosphate/ribulose-5-phosphate was also increased 1.5-fold to 2.5-fold. Both lactate and valine concentrations were increased up to 16-fold and 1.5-fold during muscle hypertrophy, respectively. Supporting the in vitro investigation presented here, serine concentration was also decreased in Cheng et al.[14] (*Figure 4A*).

Metabolic set enrichment analyses of different metabolite concentrations following muscle hypertrophy-inducing treatments revealed a significant association in the concentrations

Table 1 Design and characteristics of the individual studies (n = 8) included in the systematic review

Author (year)	Model intervention (n)	Model control (n)	Sex	Body weight	Tissue analysed	Muscle weight	Age (weeks)	Intervention	Detection method
Baumert et al. (2022)	C2C12 muscle cells	C2C12 muscle cells	NA	NA	NA	NA	5 days after different.	IGF-1 incubation	LC-MS/MS
Baumert et al. (2022)	C57BL/6 mouse (6)	C57BL/6 mouse (6)	Male	31.3 g	Plan	C: 21 mg I: 24 mg	32	Synergist ablation	LC-MS/MS
Cheng et al. (2014)	Akt1 DTG mouse (6)	C57BL/6 mouse (6)	Male	C: 38 g I: 38 g	GA	C: 180 mg I: 220 mg	12	Akt1 induction	H NMR
Collins-Hooper et al. (2015)	Mstn$^{-/-}$ mouse (Nk)	C57BL/6 mouse (Nk)	Both	C: 26 g I: 22 g	GA	C: 100 mg I: 180 mg	16	Myostatin KO	H NMR
Hoshino et al. (2020)	C2C12 muscle cells	C2C12 muscle cells	NA	NA	NA	NA	6 days after different.	EPS	CE-TOF-MS
Jiang et al. (2021)	C57BL/6 mouse (16)	C57BL/6 mouse (16)	Both	C: 26 g I: 26 g	GA	C: 0.42%[a] I: 0.50%[a]	8	Body vibration	LC-MS/MS
Weyrauch et al. (2020)	C57BL/6 mouse (7–9)	C57BL/6 mouse (7–9)	Both	27 g	Plan	C: 21 mg I: 30 mg	6	Synergist ablation	UPLC-MRM/MS
Wu et al. (2017)	Akt1 DTG mouse (Nk)	C57BL/6 mouse (Nk)	Both	C: Nk I: Nk	GA	C: 0.5%[a] I: 0.7%[a]	16	Akt1 induction	LC-MS/MS

Abbreviations: C, control; different., differentiation; EPS, electrical pulse stimulation; GA, gastrocnemius muscle; I, intervention; IGF-1, insulin-like growth factor-1; KO, gene knockout; NA, not applicable; Nk, not known; Plan, plantaris.
[a]Gastrocnemius:body weight ratio.

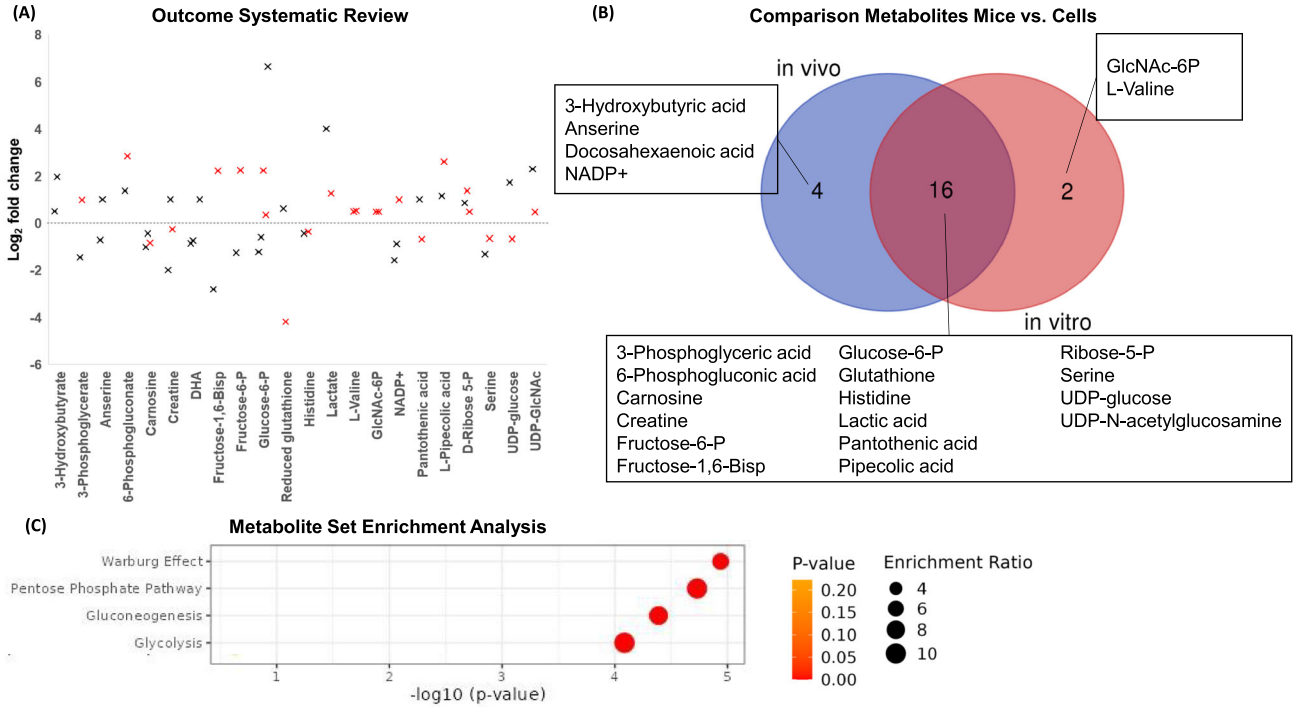

Figure 4 (A) Metabolic changes in response to skeletal muscle hypertrophy stimulation (log2 fold change vs. rest); black cross: in vivo studies; red cross: in vitro studies. (B) Venn diagram showing overlap and unique metabolites associated with muscle growth between studies performed in mice in vivo (animals) or in vitro (cell culture). (C) Enrichment analysis with MetaboAnalyst 5.0. DHA, docosahexaenoic acid; GlcNAc-6P, *N*-acetylglucosamine-6-phosphate; NADP+, oxidized nicotinamide adenine dinucleotide phosphate; P, phosphate; UDP, uridine diphosphate.

of metabolites linked to the pentose phosphate pathway, glycolysis and gluconeogenesis, all characteristic of the Warburg effect (*Figure 4C*). These results, similar to the observed changes in our muscle cells in vitro and in mice studied in vivo, further suggest that skeletal muscle hypertrophy, like in cancer, causes metabolic reprogramming to generate biomass.

[U-$^{13}C_6$]glucose tracer confirms increased amino acid carbon incorporation in insulin-like growth factor-1-stimulated C2C12 myotubes

An observation that we made in our initial studies was a shift in the concentration of glycolytic intermediates and their associated anabolic pathways (e.g., the serine synthesis pathway) during muscle hypertrophy. This observation was supported by the metabolic set enrichment analysis of the systematic review, which revealed an association with the Warburg effect. We next investigated the fate of glucose during skeletal muscle growth (*Figure 5A*). For this, we used a stable isotope [U-$^{13}C_6$]glucose tracer to identify whether stimulation with IGF-1 alters the incorporation of glucose carbon into amino acids and, ultimately, into the protein biomass of C2C12 myotubes over 24 h. Intermediary metabolism of U-$^{13}C_6$-labelled glucose results in ^{13}C-labelled carbon being incorporated into non-essential amino acids. The enrichment of ^{13}C-glucose within the conditioned media, measured in atom per cent excess (~23.5 APE), did not differ between the groups at 24 h post-tracer treatment (P = 0.95; *Figure 5A*). However, the IGF-1-treated cells showed significant additional ^{13}C-enrichment in the media lactate and alanine compared with control, suggesting that lactate and alanine were increasingly synthesized from glucose and then released into the media (*Figure 5A*). Glycine (P = 0.068) and three distinct isotopologues of proline were detected, reflecting the different routes of carbon into de novo proline synthesis (*Figure 5B*). They were also enriched with ^{13}C in the IGF-1 group within the conditioned media, respectively, reflecting the flux of glucose carbon into the non-essential amino acid pools. The enrichments were slightly higher in the IGF-1 group, possibly reflecting fluxes through de novo synthesis pathways but also inhibition of breakdown. We did not observe any ^{13}C-enrichment of serine in either the conditioned media or skeletal muscle protein. The limited ^{13}C-enrichment of serine in the media indicates that differentiated skeletal muscle cells take up more serine than they release. It also suggests that glucose-synthesized serine is rapidly utilized in downstream pathways. To ascertain whether hypertrophic muscles consume serine rather than release it, we quantified the total serine metabolite concentration in the media. Our results imply that IGF-1-treated cells potentially consume more serine

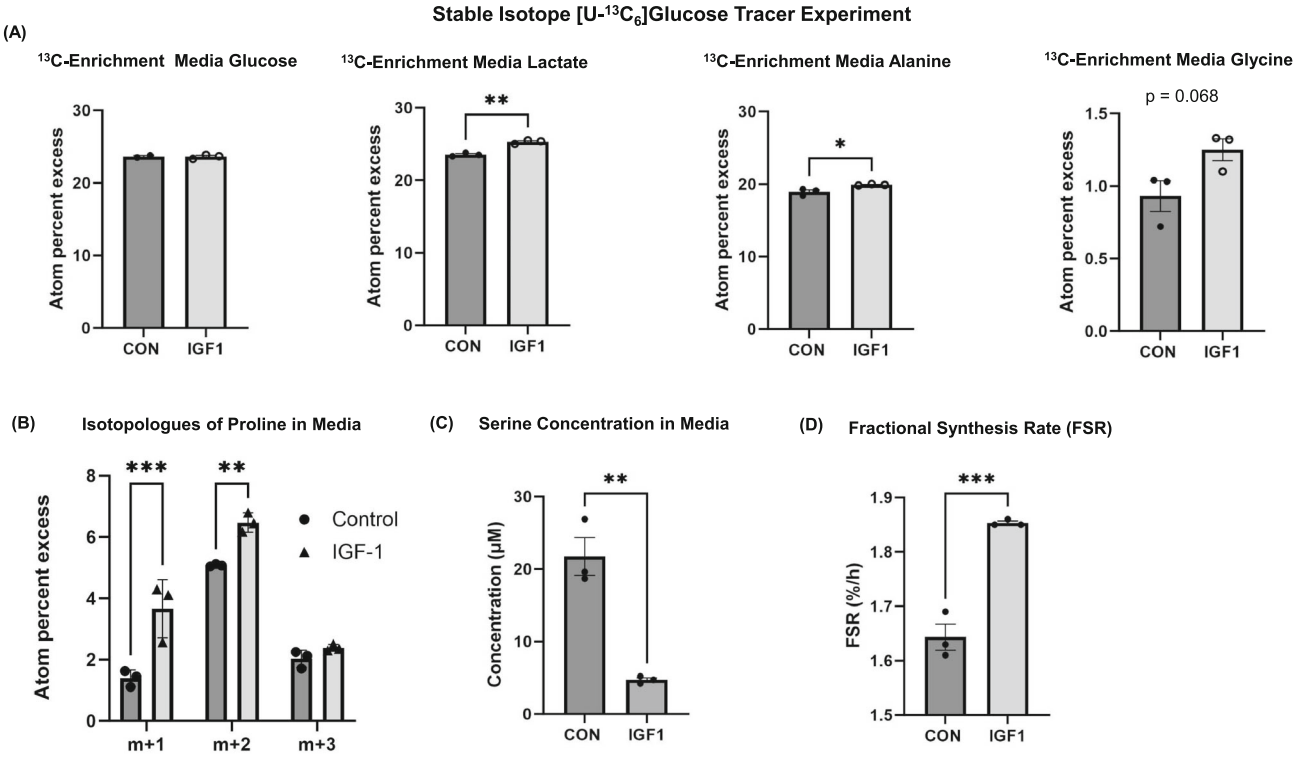

Figure 5 (A) ^{13}C-enrichment of glucose, lactate, alanine and glycine between insulin-like growth factor-1 (IGF-1) and vehicle control in conditioned media after 24 h. (B) Isotopologues of proline in media. (C) Serine concentration in conditioned media. (D) Fractional synthesis rate (FSR) based upon ^{13}C-alanine incorporation. CON, control; RAP, rapamycin. *Significant differences between groups, unpaired two-tailed Student's *t*-test ($P < 0.05$). Data are expressed as the mean ± standard error of the mean (SEM).

from the media compared with the control cells (*Figure 5C*). We then estimated the fractional rate of protein synthesis (FSR) with the ^{13}C-enriched alanine that is incorporated into muscle protein, and FSR was elevated by ~13% with IGF-1 treatment (P = 0.001; *Figure 5D*). This indicates that the ^{13}C-labelled carbon of glucose is increasingly converted to pyruvate, which is then transaminated to form alanine, which is then incorporated into proteins.

Inhibition of the key serine synthesis pathway enzyme phosphoglycerate dehydrogenase reveals a key regulatory or allowing role of the serine synthesis pathway in muscle protein synthesis

Our metabolomics in vitro study as well as the systematic review revealed a decreased serine concentration in growing muscles and an upregulation of enzymes that are linked to the serine synthesis pathway. With the stable isotope [U-$^{13}C_6$]glucose tracer, we also confirmed increased incorporation of glucose-derived carbon into glycine, suggesting that there may be increased flux through this pathway during muscle growth. Further, we recently reported that Phgdh knockdown is linked to a smaller myotube size.[16] Thus, we next inhibited Phgdh to investigate its role in muscle protein synthesis during muscle cell differentiation. Chemical inhibition of Phgdh with NCT-503 (50 μM) led to reduced protein synthesis by 58.1% ($P < 0.001$) measured by puromycin labelling (*Figure 6A*), which resulted in a 36.8% lower total muscle cell protein concentration (*Figure 6B*). Extracellular lactate dehydrogenase (LDH) activity was not changed, thus indicating that the Phgdh inhibition did not cause major cytotoxic effects (*Figure 6C*).

Collectively, these data suggest that the serine synthesis, pentose phosphate and hexosamine pathways are reprogrammed during skeletal muscle hypertrophy presumably to support biomass production, while inhibiting anabolic pathways decreases protein synthesis. Skeletal muscle converts carbon from glucose into non-essential amino acids, and the rate of incorporation increases during muscle hypertrophy.

Variants of genes involved in the serine synthesis pathway are associated with appendicular lean mass in the UK Biobank cohort

As we observed the serine synthesis pathway enzyme to regulate cell anabolism and size, we next used publicly available datasets[20] to identify three SNPs located in or near *PHGDH*, *PSPH* and *SHMT1* that are significantly associated

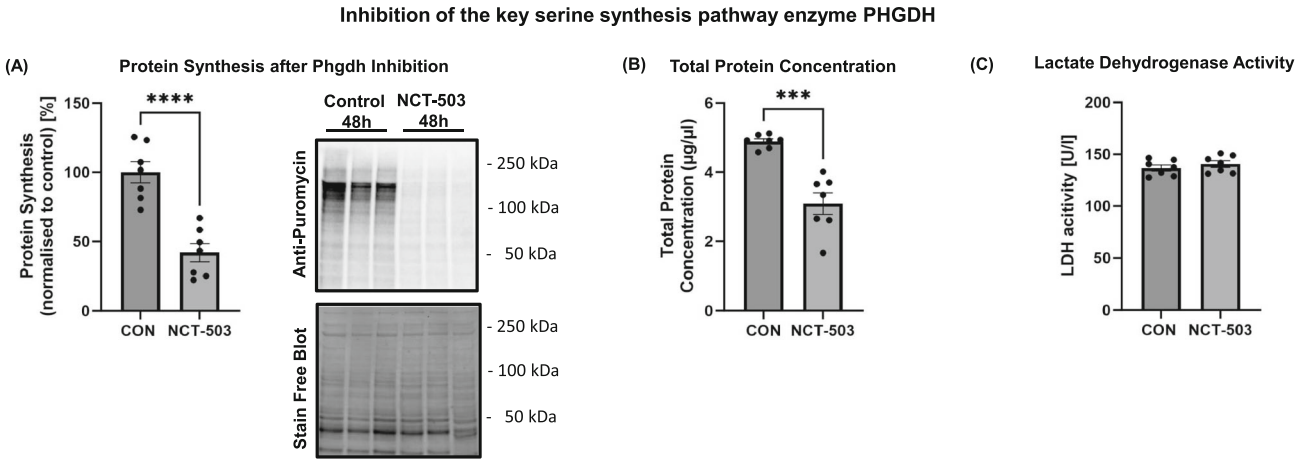

Figure 6 (A) Protein synthesis determined using puromycin; (B) total protein concentration of C2C12 myotubes; and (C) lactate dehydrogenase (LDH) activity in conditioned media measured, including NCT-503 inhibitor or vehicle control (CON) after 48 h. *Significant differences between groups, unpaired two-tailed Student's *t*-test ($P < 0.05$). Data are expressed as the mean ± standard error of the mean (SEM).

with appendicular lean mass, which is a proxy variable for muscle mass, at the genome-wide significant level ($P < 5.0e-8$) in the UK Biobank cohort (n = 450 243). More specifically, we identified an association between the *PHGDH* gene rs12129705 A (P = 1.2e-14, beta = 0.0221), the *PSPH* gene rs11982736 G (P = 9.2e-17, beta = 0.0217) and the *SHMT1* gene rs11867855 G (P = 2.9e-9, beta = 0.0132), which encodes the cytosolic form of SHMT, alleles with increased appendicular lean mass. Follow-up gene expression analysis using GTEx portal[23] revealed that these variants are functional and affect gene expression in various tissues, such as in skeletal muscle (*PSPH* rs11982736 gene variant; P = 6.8e-74) and in testis (*PHGDH* rs12129705 and *SHMT1* rs11867855 gene variants; $P < 0.0000063$).

Discussion

The major finding of this study suggests that hypertrophying skeletal muscle remodels its metabolism so that carbon from glucose increasingly diverts into anabolic pathways for building biomass. This is indicated by altered intermediate metabolite concentrations in anabolic pathways. This was further supported by stable isotope [U-$^{13}C_6$]glucose tracer experiments that indicate that labelled carbon from glucose is incorporated into the non-essential amino acid alanine in normal growing myotubes and more labelled alanine is incorporated in hypertrophying myotubes. Further mechanistic analysis revealed that the inhibition of Phgdh suppresses muscle protein synthesis in growing myotubes. This finding, coupled with GWAS analysis on appendicular lean mass in UK Biobank participants, underscores the importance of the serine synthesis pathway in muscle maintenance and potentially in preventing muscle loss.

Metabolic reprogramming

L-Carnosine and phosphorylated sugar changed their concentrations in both hypertrophied mouse muscles in vivo and cultured hypertrophying myotubes in vitro. However, the levels of phosphorylated sugar (glucose-6-phosphate, fructose-6-phosphate or glucose-1-phosphate) exhibited contrasting trends: their concentration increased in IGF-1-stimulated myotubes in vitro but decreased in overloaded muscle in vivo. Our *systematic review* also showed that the concentrations of hexose phosphates (glucose-6-phosphate, fructose-6-phosphate and fructose-1,6-bisphosphate) were consistently elevated in hypertrophying myotubes in vitro. In contrast, the majority of these concentrations exhibited a decrease in the in vivo hypertrophying mouse muscle experiments included in our review, with fructose-1,6-bisphosphate also showing a decrease after a 5-week-long resistance training regimen in healthy humans.[38] This suggests heightened metabolic activity during muscle growth, possibly due to increased demand for hexose phosphates as substrates for anabolic pathways. However, the availability of glucose and metabolites in cell culture media may not mirror in vivo conditions for (fasted) mice, prompting further exploration of dietary influences on muscle hypertrophy and metabolic reprogramming.

Of the detected amino acids, only the concentration of serine was lower in hypertrophy-simulated muscle cells. We also found that hypertrophy-stimulated muscles did not show any changes in Phgdh gene expression, the rate-limiting enzyme of the serine synthesis pathway, but had an increased expression of the *Shmt2* gene, which encodes an enzyme downstream of Phgdh. The gene encodes the serine hydroxymethyltransferase-2 enzyme that catalyses the reversible reaction of serine to glycine, thus promoting the production of one-carbon units that are indispensable for cell growth.[26] Other studies also showed a reduction of muscle

serine during muscle growth over time[14] and that C2C12 myotubes actively uptake significant quantities of serine from the media and secrete glycine in the media.[39] Therefore, the lower serine concentration in hypertrophying muscles might be due to increased activity of the serine-consuming enzyme serine hydroxymethyltransferase-2 for providing precursors for macromolecules. In support of this, we found −58.1% lower protein synthesis in Phgdh-inhibited myotubes, demonstrating that blocking the serine synthesis pathway limits protein synthesis. Further, the genetic variation data from the UK Biobank support the association between enzymes of the serine synthesis pathway (*PHGDH* and *PSPH*) and of *SHMT1* with the regulation of skeletal muscle mass. This extends beyond species-specific findings in mice, suggesting the relevance of parallel pathways of glycolysis, such as the serine synthesis pathway, to the regulation of muscle size at the population level.

We estimated with stable-isotope-labelled [U-$^{13}C_6$]glucose tracers the fractional synthesis rate of ^{13}C-enriched alanine that is incorporated into muscle protein, and the results revealed an increase of 13% in the IGF-1 group compared with the control. We also saw a small additional enrichment of carbon from glucose in the detected non-essential amino acids glycine, proline, alanine and especially lactate within the conditioned media when myotubes were stimulated with IGF-1. This suggests that the rate of incorporation of amino acids into skeletal muscle is greater during muscle growth and that the increased carbon demand for de novo biosynthesis is met by elevated glycolysis combined with a redirection of glucose intermediates towards anabolic pathways.

In addition to the serine and pentose phosphate pathways, glucose can also be directed towards the hexosamine biosynthetic pathway, resulting in the generation of UDP-sugar precursors. Our in vitro findings suggest that IGF-1 acts as an anabolic stimulus, while rapamycin serves as a catabolic stimulus, reprogramming these metabolic pathways. However, we did not observe a clear association with *O*-GlcNAcylation at either the genetic or protein level, in contrast to previous research.[28] The underlying reasons for this discrepancy remain unclear, suggesting that *O*-GlcNAcylation may not consistently change during muscle hypertrophy. Further mass spectrometry-based studies are needed to uncover more details of cellular glycosylation in the future.

Our investigation shed further light on the metabolism during muscle growth. Hypertrophying muscle rewires the metabolism, accompanied by metabolic changes in pathways associated with the Warburg effect. The results of our investigation might help to develop effective nutritional and exercise therapies against muscle wasting during ageing and metabolic diseases. Future studies should investigate whether inhibition of other key enzymes parallel to glycolysis linked with the Warburg effect[10] will further shed light on the metabolic response to muscle hypertrophy. More critically, we underscore the necessity for further studies with human participants to corroborate and expand upon our findings, potentially paving the way for practical interventions in clinical settings.

Limitations

We demonstrated a function of the serine synthesis pathway in muscle size regulation by inhibiting Phgdh with NCT-503. Further studies should use several inhibition and activation strategies in vivo for Phgdh and other key enzymes of the serine and pentose phosphate pathways. Additionally, our results of the increased Shmt2 gene expression and the relative lower metabolite concentration of serine in both muscle and conditioned media suggest an increased metabolite flux through the serine synthesis pathway. Our ^{13}C-glucose analysis allowed us to detect ^{13}C-enrichment in specific amino acids. To validate our findings, a comprehensive ^{13}C-glucose metabolic flux analysis could directly assess the metabolic flux in the serine and other pathways. The ^{13}C-enrichment in muscle protein alanine was increased. However, we have only measured FSR, and the enrichment could also reflect inhibition of muscle breakdown. Due to resource constraints, this study focused exclusively on male mice, potentially missing valuable insights into any sex-specific effects. This systematic review acknowledges a potential limitation in the comprehensiveness of its literature search. Despite our systematic and methodical approach, it is possible that not all relevant publications within the searched timeframe were identified and included. Further, we were unable to include the measurement of metabolite variation around its means due to a lack of information in some of the included publications, so our analysis is not considered meta-analysis.

Conclusions

Our results provide further evidence that muscle hypertrophy is associated with metabolic remodelling. Understanding the mechanisms regulating skeletal muscle mass can assist in developing treatments for preventing and treating muscle weakness and atrophy.

Acknowledgements

We greatly acknowledge the support of Prof. Ken Smith (School of Medicine, University of Nottingham), who processed and analysed the samples from the [U-$^{13}C_6$]glucose experiment, and of Dr Marius Garmhausen for his insightful feedback during the data analysis phase. The authors of this manuscript certify that they comply with the ethical guide-

lines for authorship and publishing in the *Journal of Cachexia, Sarcopenia and Muscle*.[40]

Open Access funding enabled and organized by Projekt DEAL.

Open Access funding enabled and organized by Projekt DEAL.

Conflict of interest statement

No conflicts of interest, financial or otherwise, are declared by the authors.

Funding

P.B., as part of the EuroTech Postdoc Program, was co-funded by the European Commission under its framework programme Horizon 2020 (Grant Agreement Number: 754462). P.B. was also supported by the TUM University Foundation Fellowship, the Company of Biologists Travelling Fellowship and the University of Jyväskylä (JYU) Visiting Fellow Program. H.W. and P.B. received grants from the Deutsche Diabetes Stiftung.

Data availability statement

The datasets that support the findings of the animal study are available as supporting information files. The human data presented in this study are publicly available online at https://genetics.opentargets.org (accessed on 20 December 2023) and https://gtexportal.org/home/index.html (accessed on 20 December 2023).

Online supplementary material

Additional supporting information may be found online in the Supporting Information section at the end of the article.

References

1. Wackerhage H, Schoenfeld BJ, Hamilton DL, Lehti M, Hulmi JJ. Stimuli and sensors that initiate skeletal muscle hypertrophy following resistance exercise. *J Appl Physiol* 2019;**126**:30–43.
2. Colberg SR, Sigal RJ, Yardley JE, Riddell MC, Dunstan DW, Dempsey PC, et al. Physical activity/exercise and diabetes: a position statement of the American Diabetes Association. *Diabetes Care* 2016;**39**:2065–2079.
3. Goodman CA. Role of mTORC1 in mechanically induced increases in translation and skeletal muscle mass. *J Appl Physiol* 2019;**127**:581–590.
4. Koopman R, Ly CH, Ryall JG. A metabolic link to skeletal muscle wasting and regeneration. *Front Physiol* 2014;**5**:32.
5. Lunt SY, Vander Heiden MG. Aerobic glycolysis: meeting the metabolic requirements of cell proliferation. *Annu Rev Cell Dev Biol* 2011;**27**:441–464.
6. Hosios AM, Hecht VC, Danai LV, Johnson MO, Rathmell JC, Steinhauser ML, et al. Amino acids rather than glucose account for the majority of cell mass in proliferating mammalian cells. *Dev Cell* 2016;**36**:540–549.
7. Possemato R, Marks KM, Shaul YD, Pacold ME, Kim D, Birsoy K, et al. Functional genomics reveal that the serine synthesis pathway is essential in breast cancer. *Nature* 2011;**476**:346–350.
8. Stincone A, Prigione A, Cramer T, Wamelink MM, Campbell K, Cheung E, et al. The return of metabolism: biochemistry and physiology of the pentose phosphate pathway. *Biol Rev* 2015;**90**:927–963.
9. Locasale JW, Grassian AR, Melman T, Lyssiotis CA, Mattaini KR, Bass AJ, et al. Phosphoglycerate dehydrogenase diverts glycolytic flux and contributes to oncogenesis. *Nat Genet* 2011;**43**:869–874.
10. Wackerhage H, Vechetti IJ, Baumert P, Gehlert S, Becker L, Jaspers RT, et al. Does a hypertrophying muscle fibre reprogramme its metabolism similar to a cancer cell? *Sports Med (Auckland, NZ)* 2022;**52**:2569–2578.
11. Brown DM, Williams H, Ryan K, Wilson T, Daniel ZC, Mareko M, et al. Mitochondrial phosphoenolpyruvate carboxykinase (PEPCK-M) and serine biosynthetic pathway genes are co-ordinately increased during anabolic agent-induced skeletal muscle growth. *Sci Rep* 2016;**6**:28693.
12. Valentino T, Figueiredo VC, Mobley CB, McCarthy JJ, Vechetti IJ Jr. Evidence of myomiR regulation of the pentose phosphate pathway during mechanical load-induced hypertrophy. *Physiol Rep* 2021;**9**:e15137.
13. Hoshino D, Kawata K, Kunida K, Hatano A, Yugi K, Wada T, et al. Trans-omic analysis reveals ROS-dependent pentose phosphate pathway activation after high-frequency electrical stimulation in C2C12 myotubes. *iScience* 2020;**23**:101558.
14. Cheng KK, Akasaki Y, Lecommandeur E, Lindsay RT, Murfitt S, Walsh K, et al. Metabolomic analysis of akt1-mediated muscle hypertrophy in models of diet-induced obesity and age-related fat accumulation. *J Proteome Res* 2015;**14**:342–352.
15. Koh J-H, Pataky MW, Dasari S, Klaus KA, Vuckovic I, Ruegsegger GN, et al. Enhancement of anaerobic glycolysis—a role of PGC-1α4 in resistance exercise. *Nat Commun* 2022;**13**:2324.
16. Stadhouders LEM, Smith JAB, Gabriel BM, Verbrugge SAJ, Hammersen TD, Kolijn D, et al. Myotube growth is associated with cancer-like metabolic reprogramming and is limited by phosphoglycerate dehydrogenase. *Exp Cell Res* 2023;113820.
17. Mäntyselkä S, Kolari K, Baumert P, Ylä-Outinen L, Kuikka L, Lahtonen S, et al. Serine synthesis pathway enzyme PHGDH is critical for muscle cell biomass, anabolic metabolism, and mTORC1 signaling. *Am J Physiol Endocrinol Metab* 2024;**326**:E73–e91.
18. Romero-Calvo I, Ocón B, Martínez-Moya P, Suárez MD, Zarzuelo A, Martínez-Augustin O, et al. Reversible Ponceau staining as a loading control alternative to actin in Western blots. *Anal Biochem* 2010;**401**:318–320.
19. Yuan M, Breitkopf SB, Yang X, Asara JM. A positive/negative ion–switching, targeted mass spectrometry–based metabolomics platform for bodily fluids, cells, and fresh and fixed tissue. *Nat Protoc* 2012;**7**:872–881.
20. Mountjoy E, Schmidt EM, Carmona M, Schwartzentruber J, Peat G, Miranda A, et al. An open approach to systematically prioritize causal variants and genes at all published human GWAS trait-associated loci. *Nat Genet* 2021;**53**:1527–1533.

21. Pei Y-F, Liu Y-Z, Yang X-L, Zhang H, Feng G-J, Wei X-T, et al. The genetic architecture of appendicular lean mass characterized by association analysis in the UK Biobank study. *Commun Biol* 2020;**3**:608.
22. Sudlow C, Gallacher J, Allen N, Beral V, Burton P, Danesh J, et al. UK biobank: an open access resource for identifying the causes of a wide range of complex diseases of middle and old age. *PLoS Med* 2015;**12**: e1001779.
23. Consortium G. Genetic effects on gene expression across human tissues. *Nature* 2017;**550**:204–213.
24. Gheller BJ, Blum JE, Lim EW, Handzlik MK, Hannah Fong EH, Ko AC, et al. Extracellular serine and glycine are required for mouse and human skeletal muscle stem and progenitor cell function. *Mol Metab* 2021; **43**:101106.
25. Buescher JM, Antoniewicz MR, Boros LG, Burgess SC, Brunengraber H, Clish CB, et al. A roadmap for interpreting ^{13}C metabolite labeling patterns from cells. *Curr Opin Biotechnol* 2015;**34**:189–201.
26. Amelio I, Cutruzzolá F, Antonov A, Agostini M, Melino G. Serine and glycine metabolism in cancer. *Trends Biochem Sci* 2014; **39**:191–198.
27. Lambert M, Bastide B, Cieniewski-Bernard C. Involvement of O-GlcNAcylation in the skeletal muscle physiology and physiopathology: focus on muscle metabolism. *Front Endocrinol (Lausanne)* 2018;**9**:9.
28. Weyrauch LA, McMillin SL, Witczak CA. Insulin resistance does not impair mechanical overload-stimulated glucose uptake, but does alter the metabolic fate of glucose in mouse muscle. *Int J Mol Sci* 2020; **21**:4715.
29. Degens H, Meessen N, Wirtz P, Binkhorst R. The development of compensatory hypertrophy in the plantaris muscle of the rat. *Ann Anatomy-Anatomischer Anzeiger* 1995;**177**:285–289.
30. Ajime TT, Serré J, Wüst RC, Burniston JG, Maes K, Janssens W, et al. The combination of smoking with vitamin D deficiency impairs skeletal muscle fiber hypertrophy in response to overload in mice. *J Appl Physiol* 2021;**131**:339–351.
31. Nielsen J, Oliver S. The next wave in metabolome analysis. *Trends Biotechnol* 2005;**23**:544–546.
32. Moher D, Shamseer L, Clarke M, Ghersi D, Liberati A, Petticrew M, et al. Preferred reporting items for systematic review and meta-analysis protocols (PRISMA-P) 2015 statement. *Syst Rev* 2015;**4**:1.
33. Collins-Hooper H, Sartori R, Giallourou N, Matsakas A, Mitchell R, Makarenkova HP, et al. Symmorphosis through dietary regulation: a combinatorial role for proteolysis, autophagy and protein synthesis in normalising muscle metabolism and function of hypertrophic mice after acute starvation. *PLoS ONE* 2015;**10**: e0120524.
34. Khodabukus A, Madden L, Prabhu NK, Koves TR, Jackman CP, Muoio DM, et al. Electrical stimulation increases hypertrophy and metabolic flux in tissue-engineered human skeletal muscle. *Biomaterials* 2019;**198**: 259–269.
35. Wu C-L, Satomi Y, Walsh K. RNA-seq and metabolomic analyses of Akt1-mediated muscle growth reveals regulation of regenerative pathways and changes in the muscle secretome. *BMC Genomics* 2017; **18**:181.
36. Fazelzadeh P, Hangelbroek RW, Tieland M, de Groot LC, Verdijk LB, Van Loon LJ, et al. The muscle metabolome differs between healthy and frail older adults. *J Proteome Res* 2016;**15**:499–509.
37. Turner DC, Gorski PP, Seaborne RA, Viggars M, Murphy M, Jarvis JC, et al. Mechanical loading of bioengineered skeletal muscle in vitro recapitulates gene expression signatures of resistance exercise in vivo. *J Cell Physiol* 2021;**236**:6534–6547.
38. Gehlert S, Weinisch P, Römisch-Margl W, Jaspers RT, Artati A, Adamski J, et al. Effects of acute and chronic resistance exercise on the skeletal muscle metabolome. *Metabolites* 2022;**12**:445.
39. Lautaoja JH, O'Connell TM, Mäntyselkä S, Peräkylä J, Kainulainen H, Pekkala S, et al. Higher glucose availability augments the metabolic responses of the C2C12 myotubes to exercise-like electrical pulse stimulation. *Am J Physiol Endocrinol Metab* 2021;**321**:E229–E245.
40. von Haehling S, Morley JE, Coats AJS, Anker SD. Ethical guidelines for publishing in the Journal of Cachexia, Sarcopenia and Muscle: update 2021. *J Cachexia Sarcopenia Muscle* 2021;**12**:2259–2261.